International Journal of **QUANTUM CHEMISTRY**

Intrinsic Reaction Coordinate: Calculation, Bifurcation, and Automated Search

Satoshi Maeda,*[a] Yu Harabuchi,[a] Yuriko Ono,[a] Tetsuya Taketsugu,*[a] and Keiji Morokuma*[b]

The intrinsic reaction coordinate (IRC) approach has been used extensively in quantum chemical analysis and prediction of the mechanism of chemical reactions. The IRC gives a unique connection from a given transition structure to local minima of the reactant and product sides. This allows for easy understanding of complicated multistep mechanisms as a set of simple elementary reaction steps. In this article, three topics concerning the IRC approach are discussed. In the first topic, the first *ab initio* study of the IRC and a recent development of an IRC calculation algorithm for enzyme reactions are introduced. In the second topic, cases are presented in which dynamical trajectories bifurcate and corresponding IRC connections can be inaccurate. In the third topic, a recent development of an automated reaction path search method and its application to systematic construction of IRC networks are described. Finally, combining these three topics, future perspectives are discussed. © 2014 Wiley Periodicals, Inc.

DOI: 10.1002/qua.24757

Introduction

Intrinsic reaction coordinate (IRC), which was proposed by Fukui in 1970 as a path of chemical reactions,[1,2] is the mass-weighted steepest descent path on the potential energy surface (PES), starting from the transition structure (TS), that is, first-order saddle point. The mass-weighted steepest descent path starting from nonstationary structures is called meta-IRC.[3] The IRC is the solution of the following differential equation,

$$\frac{d\mathbf{q}(s)}{ds} = \mathbf{v}(s) \tag{1}$$

where $\mathbf{q}$ is the mass-weighted Cartesian coordinates and s the coordinate along the IRC. The normalized tangent vector $\mathbf{v}$ of the IRC corresponds to the normal coordinate eigenvector with a negative eigenvalue at the TS with $s = 0$, and, at the other points, the unit vector parallel to the mass-weighted gradient vector $\mathbf{g}$, that is, $\mathbf{v} = -\mathbf{g}/|\mathbf{g}|$ for $s > 0$ and $\mathbf{v} = \mathbf{g}/|\mathbf{g}|$ for $s < 0$. In numerical integration of Eq. (1), $\mathbf{g}$ has to be computed repeatedly. Hence, various IRC-following algorithms have been proposed to reduce the number of gradient calculations.[4–10] With help of these algorithms, the IRC approach has been used extensively in analysis and prediction of mechanisms of a variety of chemical reactions.[11–15]

There are several merits in the IRC approach. The IRC gives a unique connection from a given TS to two local minimum structures (MINs). Geometry optimization may converge to a wrong TS if a given initial structure is not sufficiently close to the desired TS. In many theoretical studies, the IRC has been calculated to confirm whether the obtained TS is connected with two MINs for a target reaction. Moreover, once a MIN-TS-MIN connection is provided, a rate constant for a corresponding elementary step can be evaluated by the transition state theory.[16,17] It is also a practical merit that obtaining a large ensemble of trajectories is not required. The formulation of Eq. (1) with the definition of $\mathbf{v}$ was started from the classical equations of motion, assuming that at every point the nuclei have infinitesimal velocity.[1] Fukui noted that the IRC represents the vibrationless–rotationless motion path of the reacting system.[2] This formulation introduced the mass-weighted coordinates, and consideration of the mass gave an adequate representation of the atomic motion. Movement of atoms along the IRC is relatively simple owing to complete omission of vibrational and rotational motions. This allows for quick understanding of the reaction mechanisms. It is also easy to see variation of various properties, such as molecular orbitals, atomic charges, and spin densities, in the course of the reaction. For example, Fukui et al.[18,19] investigated interaction frontier orbitals along the IRC, and recently Tsuneda et al.[20] proposed a new reactivity index that can be evaluated along the IRC on the basis of accurate orbital energies obtained by the density functional theory with long-range corrected functionals.[21]

There have been considerable debates concerning drawbacks of the IRC approach. One is the instability of the IRC due to the valley-ridge inflection (VRI).[22–26] The VRI may invoke a bifurcation of a bunch of dynamical trajectories with different initial conditions into one side and the other side of the ridge, through contributions of molecular vibrations

© 2014 Wiley Periodicals, Inc.

perpendicular to the IRC tangent.[27–57] In such cases, the MIN-TS-MIN connection obtained by the IRC approach can be inaccurate. Techniques to find its indication have been proposed to notice occurrence of a bifurcation.[58–60] Cases in which dynamical trajectories considerably deviate from the IRC regions have also been reported.[61–73] This often takes place in the exit channel, where the excess kinetic energy is earned by descending the potential barrier, especially when the IRC is heavily curved.[61,64] Trajectories may circumvent even the TS region in reactions driven by collision energy or thermal kinetic energy that is much larger than the barrier height.[62,63] The dynamics called "roaming"[67–73] and "roundabout"[65,66] goes through a shallow potential valley for weakly bound complexes, and the corresponding trajectories can deviate very much from the corresponding IRC. In 1980, Miller et al.[74] and Kato and Morokuma[75] proposed a treatment that incorporates dynamical effects to the IRC with the Harmonic approximation of the PES for perpendicular directions to the IRC tangent. Miller et al.'s formulation, called reaction path Hamiltonian, has been developed further with various extensions.[76] A statistical kinetic theory for the roaming reaction has also been suggested.[77] The quantum tunneling,[78–86] which allows for the corner cutting of the IRC, can be another significant cause of deviation of the actual motion of the nuclei from the IRC. Truhlar et al.[78,79] have proposed various semiclassical tunneling models to take the quantum tunneling into account in rate calculations.

The IRC can be computed automatically using one of the IRC following algorithms,[4–10] once the corresponding TS is located. However, finding TSs is a difficult task as illustrated in an early review by Müller with two-dimensional model potentials.[87] There have been considerable efforts in development of efficient TS search techniques.[12,14,15] These techniques can be classified into three types: (1) single-ended method,[88–96] (2) coordinate driving method,[97–100] and (3) double-ended (interpolation) method.[5,101–112] Methods fall into the type (1) are called quasi-Newton methods, and can optimize a TS starting from an initial guess. Methods of the type (2) follow a minimum energy path along specified reaction variables while relaxing the others. The type (3) methods can find TSs along a path connecting given two (or more) geometries. These methods require some guesses concerning reaction mechanisms. In fact, it is difficult to study mechanisms with many unknown elementary steps using only these "targeted" methods. In establishing pathways of multistep reactions, one needs to find a network of the IRC, that is, IRC network. To uncover a complicated IRC network, a fully automated search is required. Therefore, various approaches have been proposed.[113–132] In particular, an approach that ascends the PES from a minimum to saddles using the eigenvector following method[90] would be worth specific mention.[122,123] With this approach and molecular mechanics (MM) force fields, Wales et al.[124–126] have revealed many complex IRC networks for structural transitions in atomic and molecular clusters and conformational rearrangements in peptides. Furthermore, these IRC networks have been analyzed and visualized by the disconnectivity graph approach.[133–135] Although quantum mechanical (QM)

calculations are necessary to adequately describe rearrangements of covalent bonds, obtaining IRC networks with QM calculations has not been easy due to heavy computational costs. To tackle this problem, two methods have been developed: the anharmonic downward distortion following (ADDF) method and the artificial force induced reaction (AFIR) method. The ADDF method has been applied to many gas-phase reactions and the AFIR method to more complex reactions.[127–132]

As discussed above, there have been a large number of studies concerning the IRC. In this article, we describe some of our contributions. The first topic is calculation of the IRC. Morokuma et al.[4] reported the first *ab initio* study of the IRC in 1977. This work and a recent development for efficient calculation of the IRC for large systems using QM/MM[136–141] and microiteration[142,143] methods are discussed.[144–147] Since 1993, Taketsugu et al.[28–32,52] have studied bifurcation in various reactions. Thus, bifurcation and a method to find its occurrence is the second topic. Maeda et al.[127–132] have worked on development of automated TS searching methods since 2004. Concerning this topic, a recent development of the AFIR method[129–132] is introduced with a few examples of application. Finally, future perspectives are discussed.

Calculation

The first *ab initio* study of the IRC was reported in 1977 by Morokuma and coworkers,[4] for the following two reactions.

$$HCN \rightarrow CNH \tag{2}$$

$$H^- + H_3C-H \rightarrow H-CH_3 + H^- \tag{3}$$
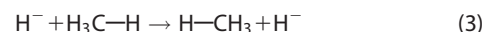
Implementation of an analytical gradient code and development of an efficient TS optimization method in their earlier study[89] were essential steps to realize these calculations. In IRC calculations, gradient vectors must be computed repeatedly. Hence, an algorithm which requires a fewer number of gradient calculations compared to the conventional Euler method was also introduced.[4] The proposed algorithm consists of two steps: a predictor step along the gradient vector, and corrector steps (energy minimization) along the bisector line of the angle between the vector along the predictor step and the gradient vector at the point which was obtained by the predictor step. With these efforts, the first *ab initio* calculation of the IRC was accomplished.[4]

Nowadays, the IRC for systems consisting of ~100 atoms is computed routinely with QM calculations. Even in very large systems such as enzyme, IRC calculations have been performed with using QM/MM approaches.[145–147] The geometrical microiteration technique, developed for efficient QM/MM geometry optimization,[142,143] can also be combined with IRC following algorithms.[144,146,147] In the microiteration, the entire system is divided into two subsystems, that is, the reaction region (R) and non reaction region (N), and atomic coordinates for the N region are optimized with fixing geometries in the R region before every displacement of atoms in the R region. In other words, the IRC is integrated in the geometrical subspace
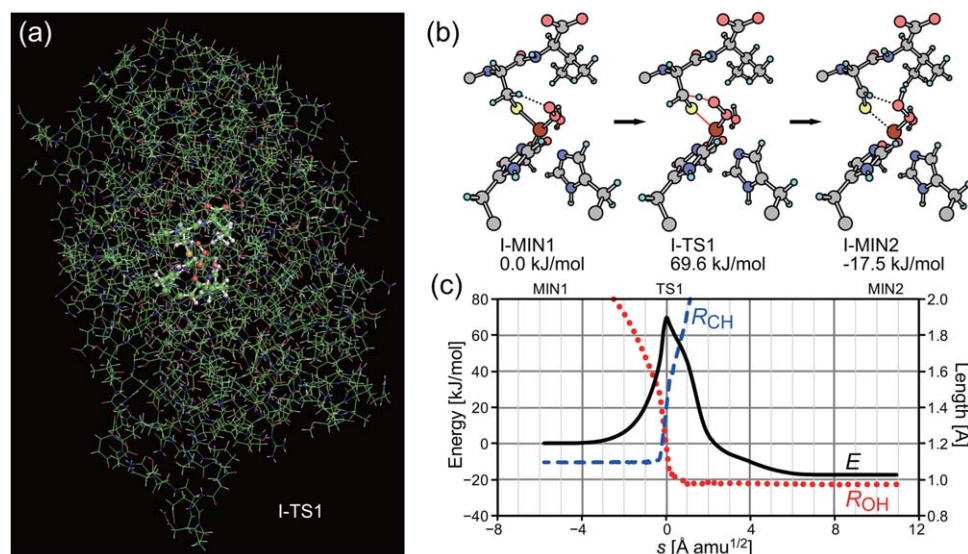
Figure 1. The μ-IRC for the first step of the isopenicillin N synthesis: a) the whole structure of the TS, b) illustrations of the reaction center structures for MIN1, TS1, and MIN2 along the μ-IRC, and c) variations of energy (solid line), C—H bond distance R_{CH} for the transferring H atom (dashed line), and O—H bond distance R_{OH} for the transferring H atom (dotted line).

fulfilling the condition $\mathbf{g}^N = \mathbf{0}$ for the gradient of the N region. As computational costs for optimization of atomic coordinates for the N part can be negligible if the N part is treated by an inexpensive MM force field and only the R part by QM calculations, total computational costs required for an IRC calculation in a large system, such as enzyme, is expected to be comparable to those for a small model system. In this approach, only complication is the representation of the Hessian, and the following effective Hessian can be adopted to take the coupling between R and N regions,

$$\frac{\partial E(\mathbf{Q})}{\partial Q_i \partial Q_j} = h_{ij}^R - \sum_{m=3p+1}^{3q} \sum_{n=3p+1}^{3q} h_{im}^C W_{nm}^N h_{nj}^C \qquad (4)$$

where $\mathbf{Q}$ is the atomic coordinates $\{Q_i\}$ for atoms in the R region, h_{ij}^R and h_{im}^C are Hessian matrix elements of the R–R block and the R–N coupling (C) block, respectively, p and q are the number of atoms in the R region and the total number of atoms, respectively, and W_{nm}^N is an inverse Hessian matrix element of the N–N block.[144] We denote this IRC determined with the geometrical microiteration as μ-IRC. The μ-IRC is an approximate solution of Eq. (1) for the full system.

Figure 1 shows an example of the μ-IRC for the initial step of isopenicillin N synthesis. This step occurs in the quintet spin state.[148] A whole image of the TS including 5368 atoms is shown in Figure 1a. The set of stationary points MIN-TS-MIN for this elementary step is presented in Figure 1b, where only atoms in the R region are shown for clarity. In ONIOM calculations,[139,141] a subsystem composed of these 65 atoms was considered to be the model system and treated by the B3LYP/ 6-31G* method, where terminal C atoms were replaced by link H atoms in the model system. For the MM part, the AMBER force field was applied. These setups are identical to those used in the previous study.[148] The μ-IRC was integrated by

the local quadratic approximation (LQA)[7] method combined with the microiteration. The LQA method requires Hessian in every integration step; it was computed analytically at every 10 step and updated by the Bofill's algorithm[149] in the other steps. In construction of the effective Hessian, matrix elements of the N–N block for atoms distant more than 10 Å from any of atoms in the R region were set zero. The step size was adjusted so that the total atomic displacement in the R region with the simple Euler step becomes 0.05 Å.

The energy profile along the μ-IRC is shown in Figure 1c with a solid line. The path coordinate s represents the sum of coordinate displacements in the R region. This profile can be decomposed into three stages: approach of the H atom in the CH_2 group to the O atom of the O_2 molecule, the H atom transfer from C to O, and conformational relaxations. The very sharp peak in a narrow path area of $-0.3 < s < 1.0$ describes the H atom transfer event. As shown also in Figure 1c, the C—H bond distance R_{CH} rises sharply around $s = -0.3$ and the O—H bond distance R_{OH} converges to ~ 0.98 Å near $s = 1.0$. After the H atom transfer, the system undergoes conformational rearrangements involving rotations of —CH=S and —O—OH groups.

The μ-IRC is an approximate solution of Eq. (1) for the full system. Nevertheless, the energy profile as well as the MIN-TS-MIN connection of the μ-IRC in Figure 1 looks reasonable. This example demonstrates that the μ-IRC approach allows for efficient computation of an approximate IRC for the large full system with a comparable computational cost to the corresponding IRC calculation in a small model system. It is noted that Thiel and coworkers[147] recently systematically compared the IRC integrated with and without the microiteration, and demonstrated that the microiteration can safely be used to check the connectivity between a TS and the associated reactant and product.
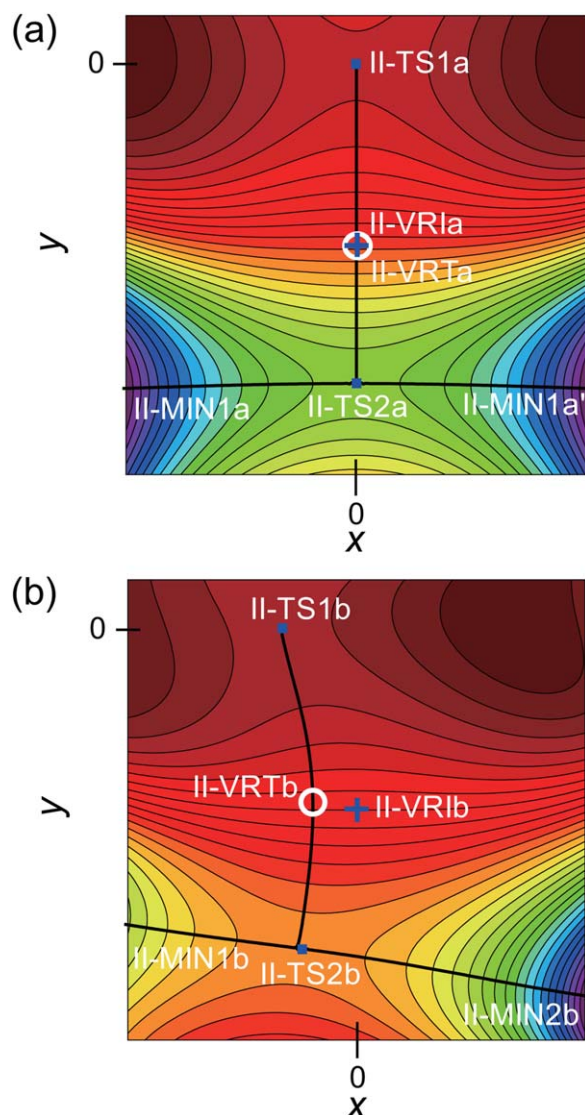
Figure 2. Schematic illustrations of the bifurcation with two-dimensional model potentials: a) a symmetric case with respect to the x-axis and b) an asymmetric case.

Bifurcation

Figure 2 illustrates bifurcations of two types with two dimensional model potentials. The potential of Figure 2a is symmetric with respect to the x-axis, and exhibits a bifurcation on a symmetric ridge. There are two TSs, II-TS1a and II-TS2a, and the IRC starting from II-TS1a reaches II-TS2a due to the symmetry. Then, the second IRC from II-TS2a leads to II-MIN1a and II-MIN1a'. There is a VRI point, II-VRIa, at which the curvature in the x axis changes from positive (valley) to negative (ridge). A bunch of dynamical trajectories starting around II-TS1a bifurcates after II-VRIa, leading to one of the potential wells, MIN1a or MIN1a', depending on initial conditions. Bifurcations of this type show an apparent indication; an IRC from a TS reaches another TS that is lower than the first TS. Moreover, finding the VRI point is relatively easy, as the VRI point is located on the IRC.

On the potential shown in Figure 2b, a bifurcation on an asymmetric ridge takes place. The IRC from II-TS1b directly leads to II-MIN1b, passing through near II-TS2b. With the IRC approach, II-MIN2b can be reached from II-MIN1b only through II-TS2b. However, dynamical trajectories starting around II-TS1b can lead to either II-MIN1b or II-MIN2b depending on initial conditions. Along the IRC, the valley-ridge transition[150] (VRT) takes place at the VRT point, VRTb, (see below for their definitions). Thus, the VRT point on the IRC can be an indication of bifurcations of this type. The real VRI point, VRIb, which is located not necessarily on the IRC, must be searched in the full dimension.[59,60] Conversely, locating the VRT point on the IRC is relatively easy as discussed below.[52]

Finding indication of bifurcation

The VRI is an $f - 2$ dimensional hyperspace that meets two conditions simultaneously:[26] (i) the second order derivative matrix $\mathbf{H}$, Hessian in terms of the mass-weighted coordinate $\mathbf{q}$ for f internal degrees of freedom, has a zero-eigenvalue normal mode and (ii) the zero-eigenvalue mode is orthogonal to the gradient vector. On the model potentials of Figure 2 with $f = 2$, the VRI is zero dimensional, that is, a point, as indicated by + marks (see II-VRIa and II-VRIb). At any nonstationary points, $\mathbf{v}$ is totally symmetric and is orthogonal to nontotally symmetric modes. If there is a point at which a nontotally symmetric mode has zero-eigenvalue on the IRC, it corresponds to a crossing point between the IRC and a VRI hyperspace, that is, a VRI point on the IRC. In Figure 2a, II-VRIa is located on the IRC, and the x- and y-axes on the plane of $x = 0$ correspond to nontotally symmetric and totally symmetric modes, respectively. In other words, a VRI point can be found on the IRC when a bifurcation takes place along a nontotally symmetric mode. In cases that a bifurcation occurs along a totally symmetric mode, which is not necessarily orthogonal to $\mathbf{v}$, the VRI hyperspace does not cross the IRC. This situation is illustrated in Figure 2b, and II-VRIb is located at a point away from the IRC.

A point on the IRC, at which a direction perpendicular to $\mathbf{v}$ has zero-curvature, may be called a VRT point.[150] Such a point can be found by normal mode analysis for directions perpendicular to $\mathbf{v}$. This can be performed by diagonalizing the projected Hessian $\mathbf{H}^{\mathrm{P}}$.[74]

$$\mathbf{H}^{\mathrm{P}} = (\mathbf{1} - \mathbf{v}\mathbf{v}^t)\mathbf{H}(\mathbf{1} - \mathbf{v}\mathbf{v}^t) \qquad (5)$$

Diagonalization of $\mathbf{H}^{\mathrm{P}}$ gives $f - 1$ eigenvectors perpendicular to $\mathbf{v}$. At the TS, all the $f - 1$ modes have positive eigenvalues. Along the IRC, one of eigenvalues may change its sign from positive to negative. The point at which the sign change occurred or the eigenvalue is zero is the VRT point. In Figure 2a, the VRT point (II-VRTa) is identical to II-VRIa due to symmetry. Conversely, in Figure 2b, II-VRTb is located on the IRC, while II-VRIb is not. As demonstrated below with two examples, occurrence of bifurcations can be suggested by locating a VRT point along the IRC.
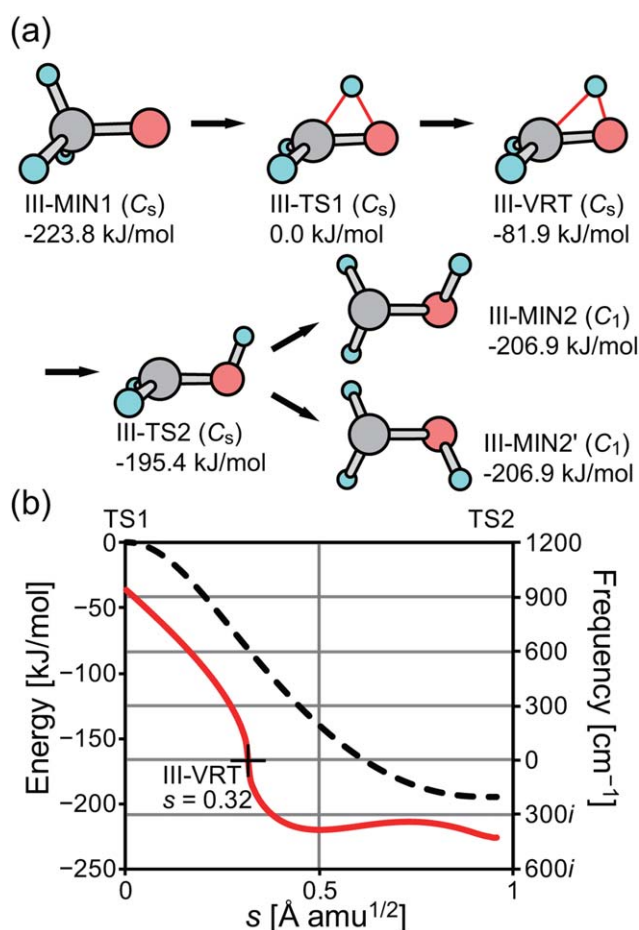
Figure 3. A bifurcation on a symmetric ridge for an isomerization of $CH_3O^\bullet$ radical: a) structures and their energies and b) variations of energy (dashed line and left-hand scale) and frequency of the lowest eigenvalue mode of $\mathbf{H}^P$ (solid line and right-hand scale) along the IRC from III-TS1.

In Figure 2b, the IRC goes through a very close vicinity of II-TS2b. Thus, the IRC from a TS passing through near another TS can be an alternative indication of a bifurcation. Finding bifurcations by looking at this indication is currently under test.

Bifurcation on symmetric ridge

Bifurcation of the symmetric case is shown in Figure 3, for an isomerization reaction of CH_3O radical. Geometry optimizations and IRC calculations were performed for this article at the UHF/6–31G** level, the same to the level used in the original paper.[29] Figure 3a shows ball-and-stick representations of TSs and MINs, and (b) variations of energy (dashed line and left-hand scale) and frequency of the lowest eigenvalue mode of $\mathbf{H}^P$ (solid line and right-hand scale) along the IRC from III-TS1. Taketsugu and Kumeda[32] performed *ab initio* molecular dynamics (AIMD) simulations, and confirmed that trajectories starting around III-TS1 bifurcate and fall down either III-MIN2 or III-MIN2′ around the ridge region deviating from the IRC.

The reactant III-MIN1 has a C_s symmetry, and the C_s symmetry is maintained along the IRC of the first step. The lowest

eigenvalue of $\mathbf{H}^P$ is positive at TS1, and decreases in the course of the reaction. At $s = 0.32$, its sign changes from positive to negative, and this point, which is illustrated as III-VRT in Figure 3a, is the VRT point. The zero-eigenvalue mode involves an out-of-plane motion of the transferring H atom from the plane of C_s symmetry, and is nontotally symmetric. Thus, III-VRT can be denoted as a VRI point as well, as both of the two conditions for VRI are fulfilled at III-VRT. The IRC reaches III-TS2, and the second IRC from III-TS2 leads to the identical products III-MIN2 and III-MIN2′. This reaction profile can be compared well with the two-dimensional model potential shown in Figure 2a.

Bifurcation on asymmetric ridge

The second example is an electron transfer reaction, $RCHO^{\bullet-} + CH_3X$, which undergoes a bifurcation on an asymmetric ridge. Bifurcation in this reaction was first suggested by Shaik et al.[38] with steepest descent path calculations. For the case with R = H and X = Cl, they found that steepest descent paths starting from a TS with two different sets of coordinates lead to different products, that is, $CH_2(CH_3)(O^\bullet) + Cl^-$ and $HCHO + {}^\bullet CH_3 + Cl^-$. This suggested that the IRC goes through a ridge region separating valleys for the two different product minima, and subtle changes in the reaction course due to the use of different coordinates resulted in paths to two different products. Yamataka et al.[39] confirmed with AIMD simulations that dynamical trajectories starting around the TS give the two products depending on initial conditions. Schlegel and coworkers[40,45,46] also performed AIMD simulations and discussed substitution and temperature effects on the branching ratio. For the case with R = H and X = Cl, Shaik et al.[38] found that along the IRC there is a ridge region at which $\mathbf{H}^P$ has a negative eigenvalue mode. Moreover, Taketsugu et al.[52] located a VRT point for the case R = CH_3 with X = Cl.

In this article, the case with R = H and X = Cl is introduced. Geometry optimizations and IRC calculations were performed at the UHF/6-31+G* level, the same to the level used in the previous AIMD study.[39] Figure 4a shows ball-and-stick representations of TSs and MINs, and (b) variations of energy (dashed line and left-hand scale) and frequency of the lowest eigenvalue mode of $\mathbf{H}^P$ (solid line and right-hand scale) along the IRC from IV-TS1. The IRC starting from IV-TS1 undergoes a C—C bond formation and a C—Cl bond cleavage giving the S_N2 product of $CH_2(CH_3)(O^\bullet) + Cl^-$. The lowest eigenvalue of $\mathbf{H}^P$ becomes negative after passing through IV-VRT at $s = 0.22$, and this suggests that a bifurcation may occur in this ridge area of $0.22 < s < 2.15$. IV-VRT rationalizes the occurrence of the trajectory bifurcation to IV-MIN2 and IV-MIN3 at the UHF/6-31+G* level.[39] We note here that on the PES at the UMP2/6-31+G* level the corresponding VRT point as well as the resulting ridge region disappear.[52] It was also found that the corresponding PES area is nearly flat toward the bifurcation direction,[52] and this may allow a small fraction of trajectories to fall down into the well of IV-MIN3 even at the UMP2 level. Further AIMD studies would be required in future with higher computational levels. A remaining problem is how to identify
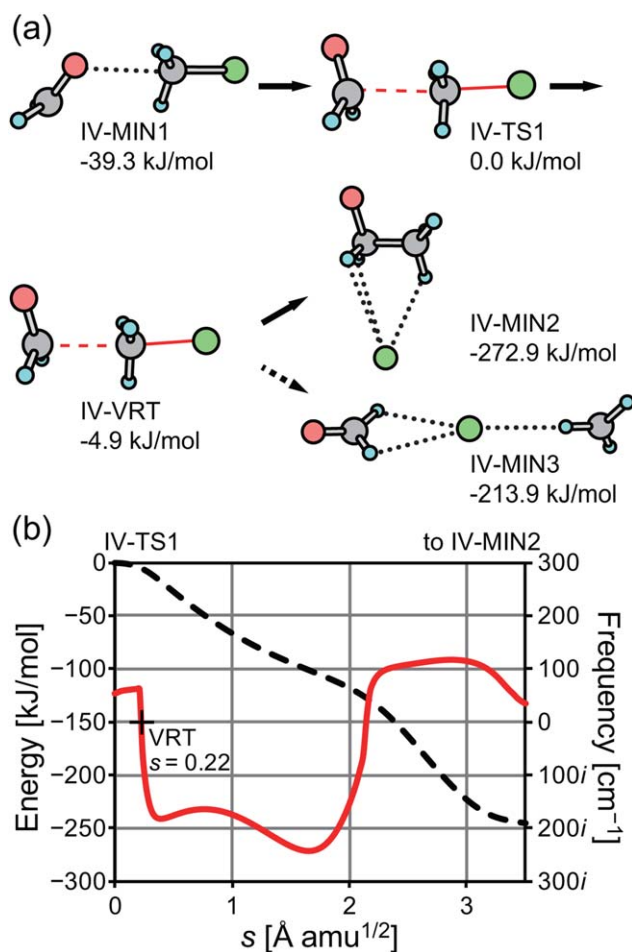
(a)

IV-MIN1
−39.3 kJ/mol

IV-TS1
0.0 kJ/mol

IV-VRT
−4.9 kJ/mol

IV-MIN2
−272.9 kJ/mol

IV-MIN3
−213.9 kJ/mol

(b)

Figure 4. A bifurcation on an asymmetric ridge for an electron transfer reaction $HCHO^{\bullet-} + CH_3Cl \rightarrow CH_2(CH_3)(O^{\bullet}) + Cl^-$ / $HCHO + {}^{\bullet}CH_3 + Cl^-$: a) structures and their energies and b) variations of energy (dashed line and left-hand scale) and frequency of the lowest eigenvalue mode of $\mathbf{H}^p$ (solid line and right-hand scale) along the IRC from IV-TS1.

the connection between the VRT point and the second product minimum (IV-MIN3 in this case) with static calculations. Although running a bunch of dynamical trajectories from the TS is one solution, it can be computationally expensive in large systems. Moreover, results of MD simulations with a limited number of trajectories are not unique and depend on initial conditions. Hence, an alternative approach defining the second connection with static calculations is under development. For obtaining branching ratios, MD simulations are required. Such a MD simulation can be performed efficiently starting either from TSs with a proper initial condition sampling at TS[66] or from reactant regions using a collective coordinate approach such as meta-dynamics.[151]

Automated Search

In this section, the AFIR method and its applications are described.[129–132] In the AFIR method, two (or more) fragments are pushed together, by minimizing the AFIR function that is composed of the adiabatic potential energy and an arti-

ficial force term.[130] When the two fragments A and B are both single atoms, although alternative choices would be possible, we adopt a very simple force term, just a linear function αr_{AB} of the interatomic distance r_{AB} with a constant parameter α. In cases that A and B are not single atoms, we adopt the following AFIR function $F(\mathbf{Q})$.

$$F(\mathbf{Q}) = E(\mathbf{Q}) + \alpha \frac{\sum_{i \in A} \sum_{j \in B} \omega_{ij} r_{ij}}{\sum_{i \in A} \sum_{j \in B} \omega_{ij}} \qquad (6)$$

In Eq. (6), $E(\mathbf{Q})$ is the potential energy that depends on the atomic coordinates $\mathbf{Q} = \{Q_k\}$ and summation of the distance r_{ij} between atoms i and j in fragments A and B, respectively, is taken with weight ω_{ij}. This weight function ω_{ij} is chosen to be,

$$\omega_{ij} = \left[\frac{(R_i + R_j)}{r_{ij}} \right]^p \qquad (7)$$

In this equation, R_i is the covalent radius for atom i, and p is set to the standard value 6. For convenience of users, α can be rewritten as follows.

$$\alpha = \frac{\gamma}{\left[2^{-\frac{1}{6}} - \left(1 + \sqrt{1 + \frac{\gamma}{\varepsilon}} \right)^{-\frac{1}{6}} \right] R_0} \qquad (8)$$

The model collision energy parameter γ is introduced in Eq. (8), and α with this equation corresponds to the mean force that acts between two Ar atoms on the Lennard-Jones potential ($R_0 = 3.8164$ Å and $\varepsilon = 1.0061$ kJ/mol) from the minimum point to the turning point in their direct collision with collision energy γ. In other words, γ provides approximate upper limit of the barrier height to be searched.

Two different algorithms have been developed. One is called multicomponent AFIR (MC-AFIR), and used for bimolecular and multicomponent reactions.[131] In MC-AFIR, at first two or more fragments are randomly placed, and then the AFIR function of Eq. (6) is minimized. The path of minimization of the AFIR function is called an AFIR path. An AFIR minimization gives an approximate product structure as a local minimum on the AFIR function, when γ is sufficiently large to overcome the barrier. The maximum point for $E(\mathbf{Q})$ along the AFIR path can be a good approximation of TS. The accurate TS and product structures are then fully optimized without artificial force from these approximate structures using any standard optimization method. By repetition of minimization of the AFIR function starting from a sufficient number of random geometries, all associative pathways with low barrier can be obtained between given reactants.

The second algorithm called single-component AFIR (SC-AFIR) was proposed very recently.[132] SC-AFIR is an algorithm for intramolecular reactions. In bimolecular and multicomponent reactions, it is natural to choose reactant molecules as the fragments A and B in Eq. (6). In SC-AFIR, fragments are systematically defined in a given molecule by an algorithm based on the bond-connectivity matrix.[132] Then, the AFIR paths are calculated for all pairs of the defined fragments within a
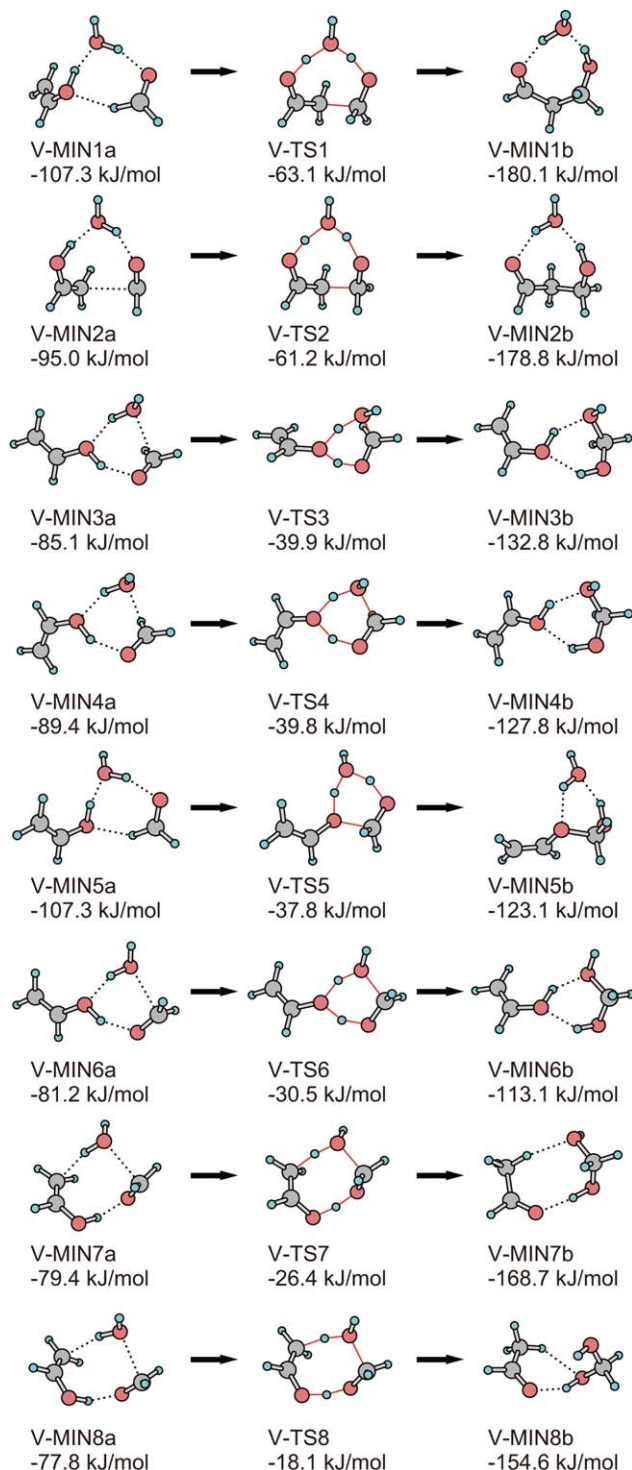
V-MIN1a −107.3 kJ/mol → **V-TS1** −63.1 kJ/mol → **V-MIN1b** −180.1 kJ/mol

V-MIN2a −95.0 kJ/mol → **V-TS2** −61.2 kJ/mol → **V-MIN2b** −178.8 kJ/mol

V-MIN3a −85.1 kJ/mol → **V-TS3** −39.9 kJ/mol → **V-MIN3b** −132.8 kJ/mol

V-MIN4a −89.4 kJ/mol → **V-TS4** −39.8 kJ/mol → **V-MIN4b** −127.8 kJ/mol

V-MIN5a −107.3 kJ/mol → **V-TS5** −37.8 kJ/mol → **V-MIN5b** −123.1 kJ/mol

V-MIN6a −81.2 kJ/mol → **V-TS6** −30.5 kJ/mol → **V-MIN6b** −113.1 kJ/mol

V-MIN7a −79.4 kJ/mol → **V-TS7** −26.4 kJ/mol → **V-MIN7b** −168.7 kJ/mol

V-MIN8a −77.8 kJ/mol → **V-TS8** −18.1 kJ/mol → **V-MIN8b** −154.6 kJ/mol

Figure 5. Paths of single water assisted reactions between HCHO and CH$_2$=CH—OH obtained by the MC-AFIR method.

certain distance. Approximate TSs obtained as highest energy points along the AFIR paths are fully optimized without artificial force by any standard optimization method. IRC calculations are made for all obtained TSs, to find the path connectivity and also to locate new MINs. By applying these procedures to all MINs or to those fulfilling certain conditions

one after another, one can construct an IRC network for a given system.

Aldol reaction

Figure 5 lists paths of single-water assisted reactions between HCHO and CH$_2$=CH—OH, obtained by an application of the MC-AFIR algorithm.[131] In this application, Eq. (6) was extended for the three component reaction as follows,

$$F(\mathbf{Q})=E(\mathbf{Q})+\frac{\alpha}{3}\left[\frac{\sum_{i\in A}\sum_{j\in B}\omega_{ij}r_{ij}}{\sum_{i\in A}\sum_{j\in B}\omega_{ij}}+\frac{\sum_{i\in A}\sum_{j\in C}\omega_{ij}r_{ij}}{\sum_{i\in A}\sum_{j\in C}\omega_{ij}}+\frac{\sum_{i\in B}\sum_{j\in C}\omega_{ij}r_{ij}}{\sum_{i\in B}\sum_{j\in C}\omega_{ij}}\right] \tag{9}$$

where HCHO, CH$_2$=CH—OH, and H$_2$O were chosen as the fragments A, B, and C, respectively. In the same way, the AFIR function can be extended for reactions involving more than three components. The parameter α was simply divided by three for the three force terms to reduce arbitrariness as much as possible, and this treatment was found to be sufficient. The B3LYP/6-31G method was adopted in this calculation. The collision energy parameter γ was set 100 kJ/mol, to find paths with barriers less than ~100 kJ/mol. In this calculation, required inputs were the computational level, the γ value, and separately optimized geometries for the three reactant molecules. With these setups, the MC-AFIR search found eight different paths, where gradient and Hessian at 13,961 and 340 geometries, respectively, were computed. It should be noted that a search with a larger γ gives many other paths with higher barriers, as discussed in a previous paper.[131] Two upper paths in Figure 5, accompanying a new C—C bond generation, exhibit relatively low barriers, and these correspond to the path of Aldol reaction.[152] The other paths leading to several byproducts were also found with higher barriers. This example demonstrates that the MC-AFIR method is powerful in identifying the best path for a given set of reactant molecules. We note that one needs to repeat MC-AFIR calculations for various combinations of molecules. Even in this simple test, reactions involving zero to two water molecules were considered one by one.[131] In practical applications, it is recommended to consider as many combinations as possible not to overlook important pathways.

Claisen rearrangement

Figure 6 shows MINs and TSs obtained by an application of the SC-AFIR method to an allyl vinyl ether CH$_2$=CH—O—CH$_2$—CH=CH$_2$.[132] The search was initiated from the most stable conformer of the reactant molecule (VI-MIN3). The SC-AFIR method was applied only to 10 conformers of the reactant molecule, that is, VI-MIN3-12, with the same bond-connectivity. In this search, the B3LYP/6–31G method was adopted, and the collision energy parameter γ was set 200 kJ/mol. Required inputs were the computational level, the γ value, and the optimized geometry of VI-MIN3. With these setups, twelve MINs and thirty-one TSs were found after
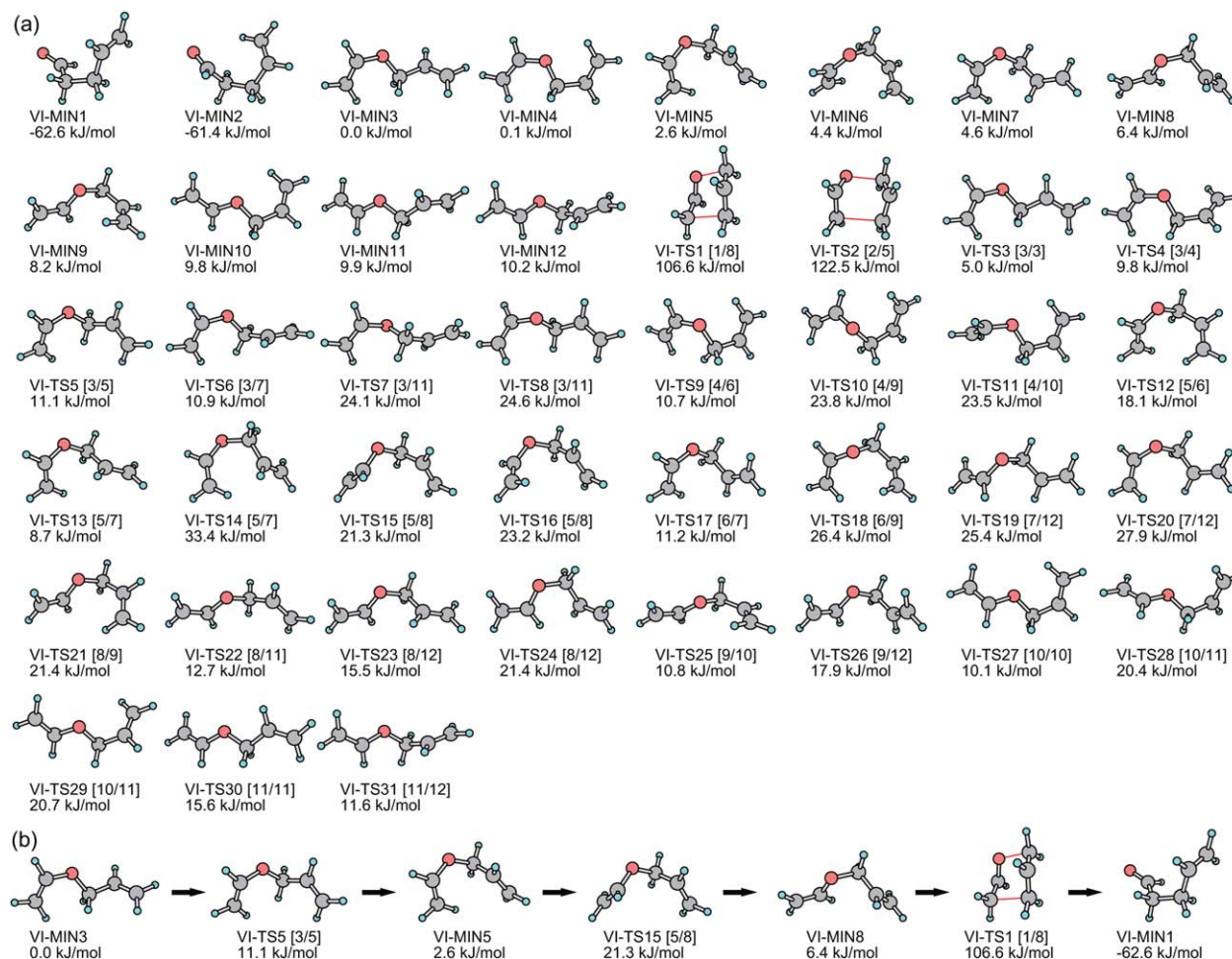
Figure 6. TSs and MINs obtained by the SC-AFIR method starting from the lowest conformer of allyl vinyl ether $CH_2{=}CH{-}O{-}CH_2{-}CH{=}CH_2$ (VI-MIN3): a) structure list and b) the best path which can be predicted on the basis of the structure list in a).

46,895 gradient and 5059 Hessian calculations. The γ value dependence of the search results is investigated in the original paper.[132] In Figure 6, many paths for conformational changes of the reactant molecule are seen. There are two bond reorganization TSs (VI-TS1 and 2), and the IRC for these TSs gave two conformers of the same carbonyl compound, that is, VI-MIN1 and 2. The best path to the carbonyl compound from VI-MIN3 is composed of three steps as illustrated in Figure 6b. This path corresponds to a well-known reaction called Claisen rearrangement.[152,153] This example demonstrates SC-AFIR method predicted the path of the real organic reaction without using any guess concerning its reaction mechanism.

Global IRC network for CH$_3$NO

The final example is a global IRC network for the molecular system with chemical formula CH_3NO. The PES of CH_3NO has been studied extensively.[154–167] However, its entire picture has not yet been available. Figure 7 shows the global IRC network for the PES of CH_3NO explored by the SC-AFIR method. The search

procedure adopted in this application is nearly identical to those used for the Claisen rearrangement in the last subsection. A difference is that the SC-AFIR method was applied to all MINs obtained in the course of the search, to see the whole PES rather than a limited area having specific bond-connectivity. The parameter γ was set 1000 kJ/mol, to cover very high energy regions of the PES as well. Moreover, the γ value was increased up to 5000 kJ/mol when a minimization of the AFIR function converged without any peak along the AFIR path. In this calculation, the B3LYP/cc-pVDZ method was adopted. The search was initiated from eight random structures. Thus, required inputs were the computational level, the γ value, and the chemical formula. Finally, 29 MINs and 135 TSs were found after 38,532 gradient and 4299 Hessian calculations. It should be noted that pathways involving biradical intermediates are not seen on this IRC network obtained by the spin-restricted calculations. Moreover, pathways connecting two dissociation channels (DCs) are not shown for clarity.

The IRC network shown in Figure 7 is highly complicated. The most stable isomer formamide (VII-MIN0) is connected directly to five isomers and four DCs. Conformers of
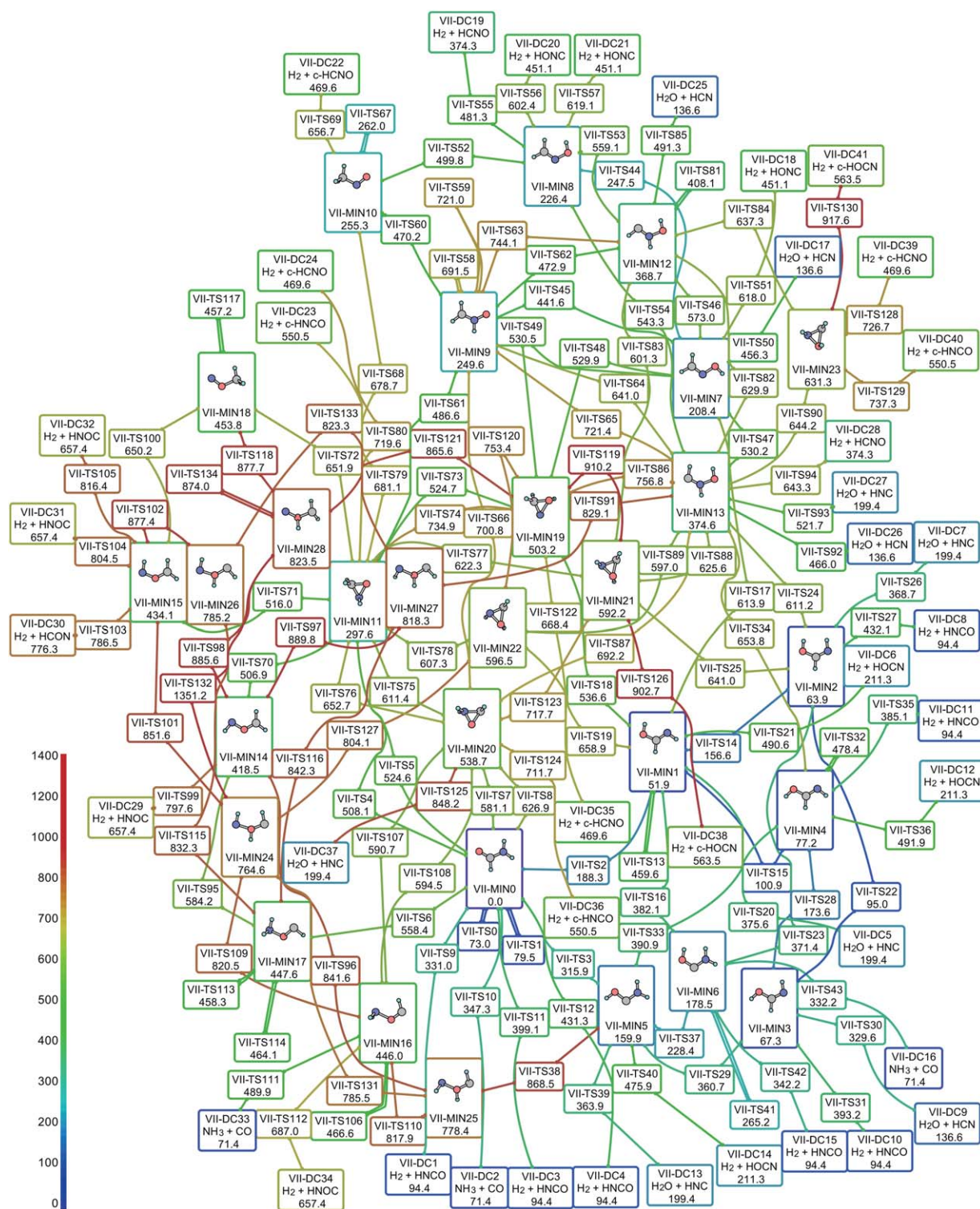
Figure 7. An IRC network for whole of the PES of CH$_3$NO obtained by the SC-AFIR method. Colors of structure flames and connection lines follow the color code which varies depending on energy values.

hydroxyimine HO—CH$_2$=NH (VII-MIN1–4) are the next stable MINs, followed by two carbene species HO—C:—NH$_2$ (VII-MIN5 and 6). These seven MINs are located in the low energy region with relative energies below 200 kJ/mol. In the range 200–300 kJ/mol, five more MINs fulfilling the octet rule are located:

conformers of CH$_2$=N—OH (VII-MIN7 and 8), CH$_2$=NH$^+$—O$^-$ (VII-MIN9), CH$_3$-N—O (VII-MIN10), and cyclic-CH$_2$NHO (VII-MIN10). Metastable species located in higher energy regions may be a transient intermediate in high energy environments such as combustion and plasma.

Summary and Perspectives

In this article, three topics concerning the IRC approach were introduced. In the first topic, the first *ab initio* study of the IRC for simple gas-phase reactions and a very recent development of the μ-IRC approach and its application to an enzyme reaction were described. A most significant role of the IRC approach is to identify the MIN-TS-MIN connection for a given TS. In the second topic, cases were discussed in which a MIN-TS-MIN connection obtained by the IRC approach can be inaccurate due to trajectory bifurcations. Finally, automated search for TSs by the MC- and SC-AFIR methods and construction of IRC networks on the PES of QM calculations were presented.

The MC- and SC-AFIR methods are implemented in a developmental version of the GRRM program,[168] and results presented in this article were obtained by the GRRM program combined with the Gaussian 09 program (GRRM/G09).[169] The μ-IRC shown in the first topic was also obtained by GRRM/G09. Data discussed in the second topic were reconstructed for this article, and these calculations including VRT point searches were made by GRRM/G09. In other words, the GRRM program can make all these analyses. Furthermore, GRRM can be combined with any electronic structure calculation program. These demonstrate usefulness of the GRRM program in analysis of chemical reaction mechanisms.

As shown in the first topic, the IRC in very large systems can be computed by the μ-IRC approach with comparable computational costs required for a small model system. The next challenge would be calculation of the IRC for enzymes on the PES with free-energy perturbation corrections concerning the motion of the MM atoms.[170–172] The effective Hessian approach introduced in the first topic allows for construction of the projected Hessian $\mathbf{H}^P$ for a defined reaction center, and the VRT search introduced in the second topic can readily be applied to the μ-IRC for finding bifurcations in enzymes. Furthermore, the AFIR method has already been combined with the QM/MM-ONIOM method and the microiteration technique,[146] and further applications are under progress.

Bifurcations have been found in many reactions by chance or by intuitive searches. The question is how many bifurcations exist on entire IRC networks obtained by automated searches. An answer can be obtained by extensive applications of the VRT point searches along available IRC networks. Such a study is in progress for small systems. Finding the second connection opened by bifurcation, that is, the path leading to the alternative product, is a remaining issue. A static approach for defining the second connection is under development. Recently, a trifurcation was suggested in the last part of the exit channel of the reaction $HCHO^{\bullet-} + CH_3Cl$.[173] Exploration of trifurcations in the other reactions is also an interesting subject.

Systematic construction of IRC networks is required for analysis and prediction of complicated reaction mechanisms. For this purpose, the AFIR method is ideally suited. Actually, the AFIR method has been applied to various organic reactions. Such IRC networks can be huge and highly complicated. For cluster structural transitions and conformational rearrange-

ments in peptide, graph theoretical approaches have been proposed and used successfully for analysis and visualization of available IRC networks.[133–135] Application of such graph theoretical approaches to IRC networks for organic and enzymatic reactions is an interesting subject. Most of the IRC connections are expected to be correct. However, as discussed above, there are cases in which IRC connections can be incorrect due to complete omission of dynamical effects. A systematic technique, which can reconstruct a path network by modifying an IRC network with adding new connections which open due to dynamical effects such as bifurcations, would be required in future, to improve reliability of quantum chemical prediction of chemical reaction mechanisms.

[1] K. Fukui, *J. Phys. Chem.* **1970**, *74*, 4161.
[2] K. Fukui, *Acc. Chem. Res.* **1981**, *14*, 363.
[3] A. Tachibana, K. Fukui, *Theor. Chim. Acta* **1978**, *49*, 321.
[4] K. Ishida, K. Morokuma, A. Komornicki, *J. Chem. Phys.* **1977**, *66*, 2153.
[5] K. Müller, L. D. Brown, *Theor. Chim. Acta* **1979**, *53*, 75.
[6] M. W. Schmidt, M. S. Gordon, M. Dupuis, *J. Am. Chem. Soc.* **1985**, *107*, 2585.
[7] M. Page, J. W. McIver, Jr., *J. Chem. Phys.* **1988**, *88*, 922.
[8] C. Gonzalez, H. B. Schlegel, *J. Chem. Phys.* **1989**, *90*, 2154.
[9] J.-Q. Sun, K. Ruedenberg, *J. Chem. Phys.* **1993**, *99*, 5257.
[10] H. P. Hratchian, H. B. Schlegel, *J. Chem. Theory Comput.* **2005**, *1*, 61.
[11] S. Niu, M. B. Hall, *Chem. Rev.* **2000**, *100*, 353.
[12] H. B. Schlegel, *J. Comput. Chem.* **2003**, *24*, 1514.
[13] T. Ziegler, J. Autschbach, *Chem. Rev.* **2005**, *105*, 2695.
[14] F. Jensen, Introduction to Computational Chemistry, 2nd ed.; Wiley: Chichester, UK, **2007**.
[15] H. B. Schlegel, *WIREs Comput. Mol. Sci.* **2011**, *1*, 790.
[16] D. G. Truhlar, B. C. Garrett, S. J. Klippenstein, *J. Phys. Chem.* **1996**, *100*, 12771.
[17] A. Fernández-Ramos, J. A. Miller, S. J. Klippenstein, D. G. Truhlar, *Chem. Rev.* **2006**, *106*, 4518.
[18] H. Fujimoto, N. Koga, K. Fukui, *J. Am. Chem. Soc.* **1981**, *103*, 7452.
[19] K. Fukui, *Science* **1981**, *218*, 747.
[20] T. Tsuneda, R. K. Singh, *J. Comput. Chem.* **2014**, *35*, 1093.
[21] H. Iikura, T. Tsuneda, T. Yanai, K. Hirao, *J. Chem. Phys.* **2001**, *115*, 3540.
[22] A. Tachibana, I. Okazaki, M. Koizumi, K. Hori, T. Yamabe, *J. Am. Chem. Soc.* **1985**, *107*, 1190.
[23] P. Valtazanos, K. Ruedenberg, *Theor. Chim. Acta* **1986**, *69*, 281.
[24] W. Quapp, *Theor. Chim. Acta* **1989**, *75*, 447.
[25] H. B. Schlegel, *J. Chem. Soc. Faraday Trans.* **1994**, *90*, 1569.
[26] W. Quapp, *J. Mol. Struct.* **2004**, *695*, 95.
[27] P. Valtazanos, S. T. Elbert, S. Xantheas, K. Ruedenberg, *Theor. Chim. Acta* **1991**, *78*, 287.
[28] T. Taketsugu, T. Hirano, *J. Chem. Phys.* **1993**, *99*, 9806.
[29] T. Taketsugu, N. Tajima, K. Hirao, *J. Chem. Phys.* **1996**, *105*, 1933.
[30] T. Yanai, T. Taketsugu, K. Hirao, *J. Chem. Phys.* **1997**, *107*, 1137.
[31] Y. Kumeda, T. Taketsugu, *J. Chem. Phys.* **2000**, *113*, 477.
[32] T. Taketsugu, Y. Kumeda, *J. Chem. Phys.* **2001**, *114*, 6973.
[33] R. M. Minyaev, D. J. Wales, *Chem. Phys. Lett.* **1994**, *218*, 413.
[34] R. M. Minyaev, D. J. Wales, *J. Phys. Chem.* **1994**, *98*, 1942.

[35] M. Hirsch, W. Quapp, D. Heidrichb, *Phys. Chem. Chem. Phys.* **1999**, *1*, 5291.

[36] W. Quapp, V. Melnikov, *Phys. Chem. Chem. Phys.* **2001**, *3*, 2735.

[37] B. Lasorne, G. Dive, D. Lauvergnat, M. Desouter-Lecomte, *J. Chem. Phys.* **2003**, *118*, 5831.

[38] S. Shaik, D. Danovich, G. N. Sastry, P. Y. Ayala, H. B. Schlegel, *J. Am. Chem. Soc.* **1997**, *119*, 9237.

[39] H. Yamataka, M. Aida, M. Dupuis, *Chem. Phys. Lett.* **1999**, *300*, 583.

[40] V. Bakken, D. Danovich, S. Shaik, H. B. Schlegel, *J. Am. Chem. Soc.* **2001**, *123*, 130.

[41] A. G. Leach, K. N. Houk, *Chem. Commun.* **2002**, 1243.

[42] D. A. Singleton, C. Hang, M. J. Szymanski, E. E. Greenwald, *J. Am. Chem. Soc.* **2003**, *125*, 1176.

[43] D. A. Singleton, C. Hang, M. J. Szymanski, M. P. Meyer, A. G. Leach, K. T. Kuwata, J. S. Chen, A. Greer, C. S. Foote, K. N. Houk, *J. Am. Chem. Soc.* **2003**, *125*, 1319.

[44] J. Limanto, K. S. Khuong, K. N. Houk, M. L. Snapper, *J. Am. Chem. Soc.* **2003**, *125*, 16310.

[45] J. Li, X. Li, S. Shaik, H. B. Schlegel, *J. Phys. Chem. A* **2004**, *108*, 8526.

[46] J. Li, S. Shaik, H. B. Schlegel, *J. Phys. Chem. A* **2006**, *110*, 2801.

[47] D. H. Ess, S. E. Wheeler, R. G. Iafe, L. Xu, N. Çelebi-Ölçüm, K. N. Houk, *Angew. Chem. Int. Ed.* **2008**, *47*, 7592.

[48] J. B. Thomas, J. R. Waas, M. Harmata, D. A. Singleton, *J. Am. Chem. Soc.* **2008**, *130*, 14544.

[49] A. N. Sheppard, O. Acevedo, *J. Am. Chem. Soc.* **2009**, *131*, 2530.

[50] T. Katori, S. Itoh, M. Sato, H. Yamataka, *J. Am. Chem. Soc.* **2010**, *132*, 3413.

[51] H. Yamataka, *Adv. Phys. Org. Chem.* **2010**, *44*, 173.

[52] Y. Harabuchi, T. Taketsugu, *Theor. Chem. Acc.* **2011**, *130*, 305.

[53] J. H. Hansen, T. M. Gregg, S. R. Ovalles, Y. Lian, J. Autschbach, H. M. L. Davies, *J. Am. Chem. Soc.* **2011**, *133*, 5076.

[54] J. Rehbein, B. K. Carpenter, *Phys. Chem. Chem. Phys.* **2011**, *13*, 20906.

[55] M. R. Siebert, P. Manikandan, R. Sun, D. J. Tantillo, W. L. Hase, *J. Chem. Theory Comput.* **2012**, *8*, 1212.

[56] B. K. Carpenter, *Chem. Rev.* **2013**, *113*, 7265.

[57] Y. J. Hong, D. J. Tantillo, *Nat. Chem.* **2014**, *6*, 104.

[58] J. Baker, P. M. W. Gill, *J. Comput. Chem.* **1988**, *9*, 465.

[59] W. Quapp, M. Hirsch, D. Heidrich, *Theor. Chem. Acc.* **1998**, *100*, 285.

[60] W. Quapp, M. Hirsch, D. Heidrich, *Theor. Chem. Acc.* **2004**, *112*, 40.

[61] L. Sun, K. Song, W. L. Hase, *Science* **2002**, *296*, 875.

[62] S. C. Ammal, H. Yamataka, M. Aida, M. Dupuis, *Science* **2003**, *299*, 1555.

[63] A. E. Pomerantz, J. P. Camden, A. S. Chiou, F. Ausfelder, N. Chawla, W. L. Hase, R. N. Zare, *J. Am. Chem. Soc.* **2005**, *127*, 16368.

[64] J. G. López, G. Vayner, U. Lourderaj, S. V. Addepalli, S. Kato, W. A. deJong, T. L. Windus, W. L. Hase, *J. Am. Chem. Soc.* **2007**, *129*, 9976.

[65] J. Mikosch, S. Trippel, C. Eichhorn, R. Otto, U. Lourderaj, J. X. Zhang, W. L. Hase, M. Weidemüller, R. Wester, *Science* **2008**, *319*, 183.

[66] M. Paranjothy, R. Sun, Y. Zhuang, W. L. Hase, *WIREs Comput. Mol. Sci.* **2013**, *3*, 296.

[67] D. Townsend, S. A. Lahankar, S. K. Lee, S. D. Chambreau, A. G. Suits, X. Zhang, J. Rheinecker, L. B. Harding, J. M. Bowman, *Science* **2004**, *306*, 1158.

[68] J. M. Bowman, X. Zhang, *Phys. Chem. Chem. Phys.* **2006**, *8*, 321.

[69] A. G. Suits, *Acc. Chem. Res.* **2008**, *41*, 873.

[70] B. R. Heazlewood, M. J. T. Jordan, S. H. Kable, T. M. Selby, D. L. Osborn, B. C. Shepler, B. J. Braams, J. M. Bowman, *Proc. Nat. Acad. Sci. USA* **2008**, *105*, 12719.

[71] N. Herath, A. G. Suits, *J. Phys. Chem. Lett.* **2011**, *2*, 642.

[72] J. M. Bowman, B. C. Shepler, *Annu. Rev. Phys. Chem.* **2011**, *62*, 531.

[73] M. P. Grubb, M. L. Warter, H.-Y. Xiao, S. Maeda, K. Morokuma, S. W. North, *Science* **2012**, *335*, 1075.

[74] W. H. Miller, N. C. Handy, J. E. Adams, *J. Chem. Phys.* **1980**, *72*, 99.

[75] S. Kato, K. Morokuma, *J. Chem. Phys.* **1980**, *73*, 3900.

[76] E. Kraka, *WIREs Comput. Mol. Sci.* **2011**, *1*, 531.

[77] S. J. Klippenstein, Y. Georgievskii, L. B. Harding, *J. Phys. Chem. A* **2011**, *115*, 14370.

[78] D. G. Truhlar, B. C. Garrett, *Acc. Chem. Res.* **1980**, *13*, 440.

[79] D. G. Truhlar, R. Steckler, M. S. Gordon, *Chem. Rev.* **1987**, *87*, 217.

[80] N. Makri, W. H. Miller, *J. Chem. Phys.* **1989**, *91*, 4026.

[81] N. Shida, J. E. Almlof, P. F. Barbara, *J. Chem. Phys.* **1991**, *95*, 10457.

[82] M. Ben-Num, T. J. Martinez, *J. Phys. Chem. A* **1999**, *103*, 6055.

[83] T. Taketsugu, N. Watanabe, K. Hirao, *J. Chem. Phys.* **1999**, *111*, 3410.

[84] G. Mil'nikov, K. Yagi, T. Taketsugu, H. Nakamura, K. Hirao, *J. Chem. Phys.* **2004**, *120*, 5036.

[85] G. Mil'nikov, H. Nakamura, *Phys. Chem. Chem. Phys.* **2008**, *10*, 1374.

[86] Y. Ootani, T. Taketsugu, *J. Comput. Chem.* **2011**, *33*, 60.

[87] K. Müller, *Angew. Chem. Int. Ed.* **1980**, *19*, 1.

[88] J. W. McIver, Jr., A. Komornicki, *J. Am. Chem. Soc.* **1972**, *94*, 2625.

[89] A. Komornicki, K. Ishida, K. Morokuma, *Chem. Phys. Lett.* **1977**, *45*, 595.

[90] C. J. Cerjan, W. H. Miller, *J. Chem. Phys.* **1981**, *75*, 2800.

[91] H. B. Schlegel, *J. Comput. Chem.* **1982**, *3*, 214.

[92] J. T. Golab, D. L. Yeager, P. Jørgensen, *Chem. Phys.* **1983**, *78*, 175.

[93] A. Banerjee, N. Adams, J. Simons, R. Shepard, *J. Phys. Chem.* **1985**, *89*, 52.

[94] T. Helgaker, *Chem. Phys. Lett.* **1991**, *182*, 503.

[95] P. Culot, G. Dive, V. H. Nguyen, J. M. Ghuysen, *Theor. Chim. Acta* **1992**, *82*, 189.

[96] Ö. Farkas, H. B. Schlegel, *J. Chem. Phys.* **1999**, *111*, 10806.

[97] D. M. Hayes, K. Morokuma, *Chem. Phys. Lett.* **1972**, *12*, 539.

[98] R. L. Jaffe, D. M. Hayes, K. Morokuma, *J. Chem. Phys.* **1974**, *60*, 5108.

[99] S. K. Burger, P. W. Ayers, *J. Chem. Theory Comput.* **2010**, *6*, 1490.

[100] C. Shang, Z.-P. Liu, *J. Chem. Theory Comput.* **2012**, *8*, 2215.

[101] T. A. Halgren, W. N. Lipscomb, *Chem. Phys. Lett.* **1977**, *49*, 225.

[102] M. J. S. Dewar, E. F. Healy, J. J. P. Stewart, J. Chem. Soc., *Faraday Trans. 2* **1984**, *80*, 227.

[103] R. Elber, M. Karplus, *Chem. Phys. Lett.* **1987**, *139*, 375.

[104] C. Choi, R. Elber, *J. Chem. Phys.* **1991**, *94*, 751.

[105] V. Ionova, E. A. Carter, *J. Chem. Phys.* **1993**, *98*, 6377.

[106] G. Henkelman, B. P. Uberuaga, H. Jónsson, *J. Chem. Phys.* **2000**, *113*, 9901.

[107] W. E, W. Ren, E. Vanden-Eijnden, *Phys. Rev. B* **2002**, *66*, 052301.

[108] P. T. Olsen, F. Jensen, *J. Chem. Phys.* **2003**, *118*, 3523.

[109] B. Peters, A. Heyden, A. T. Bell, A. Chakraborty, *J. Chem. Phys.* **2004**, *120*, 7877.

[110] S. Maeda, K. Ohno, *Chem. Phys. Lett.* **2005**, *404*, 95.

[111] S. Maeda, K. Ohno, *J. Chem. Phys.* **2006**, *124*, 174306.

[112] X.-J. Zhang, C. Shang, Z.-P. Liu, *J. Chem. Theory Comput.* **2013**, *9*, 5745.

[113] J.-Q. Sun, K. Ruedenberg, *J. Chem. Phys.* **1993**, *98*, 9707.

[114] Y. Abashkin, N. Russo, *J. Chem. Phys.* **1994**, *100*, 4477.

[115] Bondensgård, F. Jensen, *J. Chem. Phys.* **1996**, *104*, 8025.

[116] W. Quapp, M. Hirsch, O. Imig, D. Heidrich, *J. Comput. Chem.* **1998**, *19*, 1087.

[117] M. Černohorský, S. Kettou, J. Koča, *J. Chem. Inf. Comput. Sci.* **1999**, *39*, 705.

[118] K. M. Westerberg, C. A. Floudas, *J. Chem. Phys.* **1999**, *110*, 9259.

[119] K. K. Irikura, R. D. Johnson, III, *J. Phys. Chem. A* **2000**, *104*, 2191.

[120] E. M. Müller, A. de Meijere, H. Grubmüller, *J. Chem. Phys.* **2002**, *116*, 897.

[121] P. M. Zimmerman, *J. Comput. Chem.* **2013**, *34*, 3043.

[122] H. L. Davis, D. J. Wales, R. S. Berry, *J. Chem. Phys.* **1990**, *92*, 4308.

[123] C. J. Tsai, K. D. Jordan, *J. Phys. Chem.* **1993**, *97*, 11227.

[124] J. P. K. Doye, D. J. Wales, *Z. Phys. D* **1997**, *40*, 194.

[125] D. J. Wales, J. P. K. Doye, M. A. Miller, P. N. Mortenson, T. R. Walsh, *Adv. Chem. Phys.* **2000**, *115*, 1.

[126] D. J. Wales, *Int. Rev. Phys. Chem.* **2006**, *25*, 237.

[127] K. Ohno, S. Maeda, *Chem. Phys. Lett.* **2004**, *384*, 277.

[128] S. Maeda, K. Ohno, *J. Phys. Chem. A* **2005**, *109*, 5742.

[129] S. Maeda, K. Ohno, K. Morokuma, *Phys. Chem. Chem. Phys.* **2013**, *15*, 3683.

[130] S. Maeda, K. Morokuma, *J. Chem. Phys.* **2010**, *132*, 241102.

[131] S. Maeda, K. Morokuma, *J. Chem. Theory Comput.* **2011**, *7*, 2335.

[132] S. Maeda, T. Taketsugu, K. Morokuma, *J. Comput. Chem.* **2014**, *35*, 166.

[133] O. M. Becker, M. Karplus, *J. Chem. Phys.* **1997**, *106*, 1495.

[134] D. J. Wales, M. A. Miller, T. R. Walsh, *Nature* **1998**, *394*, 753.

[135] D. J. Wales, T. V. Bogdan, *J. Phys. Chem. B* **2006**, *110*, 20765.

[136] A. Warshel, M. Levitt, *J. Mol. Biol.* **1976**, *103*, 227.

[137] U. C. Singh, P. A. Kollman, *J. Comput. Chem.* **1986**, *7*, 718.

[138] M. J. Field, P. A. Bash, M. Karplus, *J. Comput. Chem.* **1990**, *11*, 700.

[139] F. Maseras, K. Morokuma, *J. Comput. Chem.* **1995**, *16*, 1170.

[140] H. M. Senn, W. Thiel, *Angew. Chem. Int. Ed.* **2009**, *48*, 1198.

[141] L. W. Chung, H. Hirao, X. Li, K. Morokuma, *WIREs Comput. Mol. Sci.* **2012**, *2*, 327.

[142] T. Vreven, K. Morokuma, Ö. Farkas, H. B. Schlegel, M. J. Frisch, *J. Comput. Chem.* **2003**, *24*, 760.

[143] T. Vreven, M. J. Frisch, K. N. Kudin, H. B. Schlegel, K. Morokuma, *Mol. Phys.* **2006**, *104*, 701.

[144] S. Maeda, K. Ohno, K. Morokuma, *J. Chem. Theory Comput.* **2009**, *5*, 2734.

[145] H. P. Hratchian, M. J. Frisch, *J. Chem. Phys.* **2011**, *134*, 204103.

[146] S. Maeda, E. Abe, M. Hatanaka, T. Taketsugu, K. Morokuma, *J. Chem. Theory Comput.* **2012**, *8*, 5058.

[147] I. Polyak, E. Boulanger, K. Sen, W. Thiel, *Phys. Chem. Chem. Phys.* **2013**, *15*, 14188.

[148] M. Lundberg, T. Kawatsu, T. Vreven, M. J. Frisch, K. Morokuma, *J. Chem. Theory Comput.* **2009**, *5*, 222.

[149] J. M. Bofill, *J. Comput. Chem.* **1994**, *15*, 1.

[150] J. M. Bofill, W. Quapp, *J. Math. Chem.* **2013**, *51*, 1099.

[151] A. Barducci, M. Bonomi and M. Parrinello, *WIREs Comput. Mol. Sci.* **2011**, *1*, 826.

[152] L. Kürti, B. Czakó, Strategic Applications of Named Reactions in Organic Synthesis; Elsevier B.V.: Amsterdam, **2005**.

[153] R. L. Vance, N. G. Rondan, K. N. Houk, F. Jensen, W. Thatcher Borden, A. Komornicki, E. Wimmer, *J. Am. Chem. Soc.* **1988**, *110*, 2314.

[154] L. Radom, N. V. Riggs, *Aust. J. Chem.* **1980**, *33*, 249.

[155] H. B. Schlegel, P. Gund, E. M. Fluder, *J. Am. Chem. Soc.* **1982**, *104*, 5347.

[156] T. Kskumoto, K. Saito, A. Imamura, *J. Phys. Chem.* **1985**, *89*, 2286.

[157] X.-C. Wang, J. Nichols, M. Feyereisen, M. Gutowski, J. Boatz, A. D. J. Haymet, J. Simons, *J. Phys. Chem.* **1991**, *95*, 10419.

[158] A. L. Sobolewski, *J. Photochem. Photobiol. A: Chem.* **1995**, *89*, 89.

[159] M. T. Nguyen, D. Sengupta, L. G. Vanquickenborne, *J. Phys. Chem.* **1996**, *100*, 10956.

[160] J. M. Martell, H. T. Yu, J. D. Goddard, *Mol. Phys.* **1997**, *92*, 497.

[161] D. Liu, W.-H. Fang, X.-Y. Fu, *Chem. Phys. Lett.* **2000**, *318*, 291.

[162] D. Du, A. Fu, Z. Zhou, *Int. J. Quant. Chem.* **2004**, *99*, 1.

[163] F. Duvernay, A. Trivella, F. Borget, S. Coussan, J.-P. Aycard, T. Chiavassa, *J. Phys. Chem. A* **2005**, *109*, 11155.

[164] M. Eckert-Maksić, M. Vazdar, M. Ruckenbauer, M. Barbatti, T. Müller, H. Lischka, *Phys. Chem. Chem. Phys.* **2010**, *12*, 12719.

[165] V. S. Nguyen, H. L. Abbott, M. M. Dawley, T. M. Orlando, J. Leszczynski, M. T. Nguyen, *J. Phys. Chem. A* **2011**, *115*, 841.

[166] M. Ferus, P. Kubelík, S. Civiš, *J. Phys. Chem. A* **2011**, *115*, 12132.

[167] M. Ferus, R. Michalčíkova̍, V. Shestivska̍, J. Šponer, J. E. Šponer, S. Civiš, *J. Phys. Chem. A* **2014**, *118*, 719.

[168] S. Maeda, Y. Osada, Y. Harabuchi, T. Taketsugu, K. Morokuma, K. Ohno, GRRM, a Developmental Version at Hokkaido University.

[169] M. J. Frisch, G. W. Trucks, H. B. Schlegel, G. E. Scuseria, M. A. Robb, J. R. Cheeseman, G. Scalmani, V. Barone, B. Mennucci, G. A. Petersson, H. Nakatsuji, M. Caricato, X. Li, H. P. Hratchian, A. F. Izmaylov, J. Bloino, G. Zheng, J. L. Sonnenberg, M. Hada, M. Ehara, K. Toyota, R. Fukuda, J. Hasegawa, M. Ishida, T. Nakajima, Y. Honda, O. Kitao, H. Nakai, T. Vreven, J. A. Montgomery, Jr., J. E. Peralta, F. Ogliaro, M. Bearpark, J. J. Heyd, E. Brothers, K. N. Kudin, V. N. Staroverov, R. Kobayashi, J. Normand, K. Raghavachari, A. Rendell, J. C. Burant, S. S. Iyengar, J. Tomasi, M. Cossi, N. Rega, J. M. Millam, M. Klene, J. E. Knox, J. B. Cross, V. Bakken, C. Adamo, J. Jaramillo, R. Gomperts, R. E. Stratmann, O. Yazyev, A. J. Austin, R. Cammi, C. Pomelli, J. W. Ochterski, R. L. Martin, K. Morokuma, V. G. Zakrzewski, G. A. Voth, P. Salvador, J. J. Dannenberg, S. Dapprich, A. D. Daniels, Ö. Farkas, J. B. Foresman, J. V. Ortiz, J. Cioslowski, D. J. Fox, Gaussian 09, Revision B.01; Gaussian, Inc.: Wallingford CT, **2009**.

[170] H. Hirao, Y. Nagae, M. Nagaoka, *Chem. Phys. Lett.* **2001**, *348*, 350.

[171] H. Hu, W. Yang, *Annu. Rev. Phys. Chem.* **2008**, *59*, 573.

[172] T. Kosugi, S. Hayashi, *J. Chem. Theory Comput.* **2012**, *8*, 322.

[173] Y. Harabuchi, A. Nakayama, T. Taketsugu, *Comput. Theor. Chem.* **2012**, *1000*, 70.